Control of the Molecular Packing in Guanidinium Monolayers through Binding with Aqueous Polycarboxylates

Ayumi Kamino, Hiroshi Koyano, Katsuhiko Ariga, and Toyoki Kunitake*,#

Supermolecules Project, JRDC, Kurume Research Center, 2432 Aikawa, Kurume, Fukuoka 839

(Received July 11, 1996)

By using newly developed guanylating agents, octadecyl- and dioctadecylguanidinium amphiphiles were synthesized. The interaction between each guanidinium monolayer and polycarboxylates in the subphase was investigated on the basis of the π–A isotherm, FT-IR spectroscopy, and XPS measurements. When linear dicarboxylates were used, the molecular areas of the monolayer increased, as the length of the methylene chain between the carboxylate groups increased. The expansion of the molecular area was greater for the octadecylguanidinium monolayers than for the dioctadecylguanidinium monolayers. The molecular packing was affected by the shape of polycarboxylate molecules in the case of phthalate, *cis*-1,2-cyclohexanedicarboxylate, and 1,1-cyclohexanediacetate. It is clear that, the molecular packing in the complexed monolayers is governed by the distance and relative orientation of the two carboxylate groups in a polycarboxylate. With all of the dicarboxylates, excluding oxalate, FT-IR and XPS measurements of the LB films indicated the formation of 1 : 1 guanidinium/carboxylate pairs with hydrogen bonding interactions. Oxalate produced an asymmetric complex where one guanidinium was bound to oxalate through hydrogen bonding, and the other guanidinium existed as a non-hydrogen bonded counter ion. These results are useful for the development of two-dimensional molecular patterns.

Molecular assemblies[1—3] are most frequently formed through weak interactions among component molecules. The control of the molecular disposition within molecular assemblies is a most important target in studying molecular assembling techniques. In the Langmuir–Blodgett (LB) technique, ultra-thin films are formed by transferring monomolecular films of lipids from a water surface onto a solid substrate.[4,5] The layer-by-layer transfer process produces films having a well-defined thickness where the distance between the functional groups and the ordering of molecules are controllable to molecular precision in the direction of the film thickness. However, the traditional LB technique cannot be effective for controlling the molecular arrangement within a two-dimensional plane. A new strategy must be added to the conventional LB technique, in order to achieve the designed molecular arrangement within a unit layer.

We have been studying molecular recognition at the air-water interface.[6—11] In these systems, host monolayers can bind aqueous guest molecules through complementary hydrogen bonding. By using multi-functional components, it becomes possible to prepare specific pairs in which the component molecules are aligned in fixed arrangements at the interface. For example, we have demonstrated that flavin adenine dinucleotide (FAD) can bind three kinds of monolayer components specifically.[12] The formation of a regular molecular pattern from the mixed monolayer and FAD has been confirmed by atomic force microscopic (AFM) observations.[13] This result may be extended more generally as a means for the formation of molecular patterns within monomolecular layers. Efficient and specific binding between a host and a guest is essential for molecular disposition within a mixed monolayer to be fixed at the air-water interface. Very strong binding constants (10^6—10^7 M^{-1}) were observed between a guanidinium monolayer and phosphate derivatives, such as AMP or ATP (1 M=1 mol dm^{-3}).[6] The interaction between guanidinium and carboxylate (see Scheme 1) would be similarly effective.[14]

In order to establish interfacial guest binding as a general methodology for molecular patterning, we need to examine the binding of a host and a guest with large structural variety. We therefore decided to use polycarboxylate as a water-soluble guest molecule, since various polycarboxylic acids, such as shown in Chart 1, are readily available.

In this study, we newly synthesized three kinds of guanidinium amphiphiles (MG, DG(C_1) and DG(C_4)), and investigated their interactions with polycarboxylates in subphase by a π–A isotherm, FT-IR spectra, and XPS measurements.

Experimental

Materials. The polycarboxylic acids used in this study are shown in Chart 1. All of the polycarboxylic acids were commercially supplied and used without purification: oxalic acid, malonic

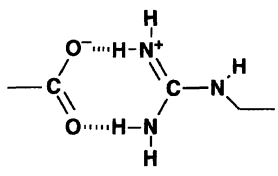

Scheme 1.

Permanent address: Faculty of Engineering, Kyushu University, Fukuoka 812.

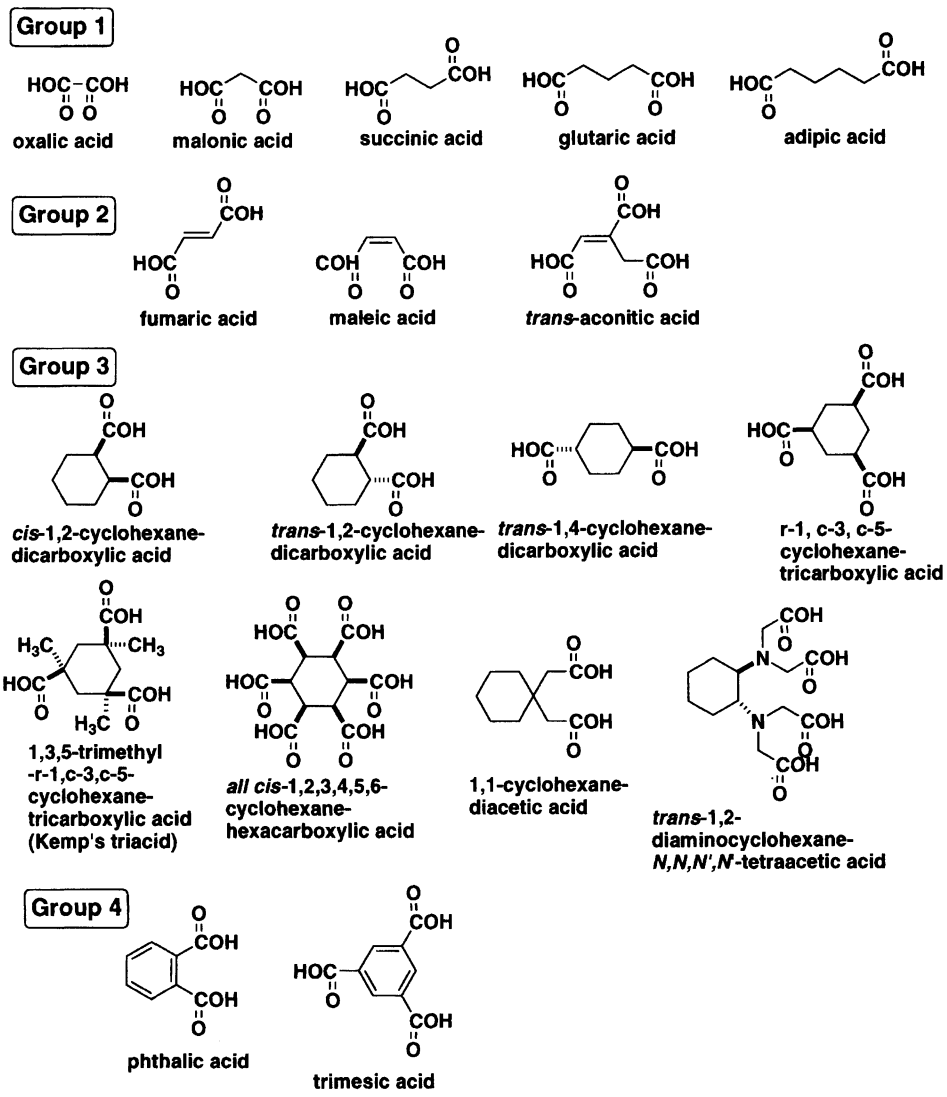

Chart 1.

acid, glutaric acid, adipic acid, *trans*-aconitic acid, 1,1-cyclohexanediacetic acid, *trans*-1,2-diaminocyclohexane-*N*,*N*,*N*′,*N*′-tetraacetic acid, phthalic acid, trimesic acid (Wako Pure Chem.), and succinic acid, fumaric acid, maleic acid (Kishida Chem.), *cis*-1,2-cyclohexanedicarboxylic acid, *trans*-1,2-cyclohexanedicarboxylic acid, *trans*-1,4-cyclohexanedicarboxylic acid (Tokyo Kasei), and r-1,c-3,c-5-cyclohexanetricarboxylic acid, 1,3,5-trimethyl-r-1,c-3,c-5-cyclohexanecarboxylic acid (Kemp's triacid), *all cis*-1,2,3,4,5,6-cyclohexanehexacarboxylic acid (Aldrich). Sodium hydroxide volumetric standard (2.0 M, in water) was also commercially supplied (Wako Pure Chem.). The water used for the subphase was deionized and doubly distilled by a Nanopure II-4P and Glass Still D44 System (Barnstead). Spectroscopic-grade benzene and ethanol (Wako Pure Chem.) were used as spreading solvents. Gold (99.999%) and chromium (99.99%) used for the surface modification of substrates were purchased from Soekawa Chemicals.

Syntheses of Guanidinium Amphiphiles. The syntheses of the guanidinium amphiphiles (MG, DG(C_1), and DG(C_4)) were performed according to the scheme of Chart 2. Anhydrous *p*-toluenesulfonic acid (TsOH) was obtained from its monohydrate by azeotropic removal of water with toluene, followed by recrystallization from ethyl acetate.[15] LiH (95%, 30 mesh) was obtained from Aldrich.

The melting points were recorded on a Yanaco micro-melting-point apparatus and are uncorrected. The chemical shifts of the ^{1}H NMR spectra were recorded on a Bruker ARX-300 (300 MHz) spectrometer, and reported relative to chloroform (δ = 7.26) or tetramethylsilane (δ = 0.00). Elemental analyses (C, H, and N) were performed at the Faculty of Science, Kyushu University.

3,5-Dimethylpyrazole-1-(*N*-benzyloxycarbonyl)carboxamidine. 3,5-Dimethylpyrazole-1-carboxyamidine nitrate is commercially available (Aldrich) and readily prepared from aminoguanidine nitrate (Aldrich) and 2,4-pentanedione in 66% yield according to the literature.[16] A mixture of 3,5-dimethylpyrazole-1-carboxamidine nitrate (10.0 g, 49.7 mmol), benzyl chloroformate (8.35 g, 50.0 mmol), and triethylamine (10.1 g, 100 mmol) in CH_2Cl_2 (130 mL) was stirred at room temperature for 16 h. This was washed with water (×2) and brine. After being dried over Na_2SO_4, the organic layer was concentrated under reduced pressure to give a solid, which was recrystallized from CH_2Cl_2/hexane to give the title compound (10.9 g, 80%) as a colorless powder. Mp 95.0—95.6 °C; TLC R_f 0.47 (4 : 1 hexane/ethyl acetate); ^{1}H NMR ($CDCl_3$) δ = 2.22 (3H, s, CH_3), 2.64 (3H, s, CH_3), 5.21 (2H, s, CH_2O), 5.95 (1H, s, vinyl), 7.3—7.4 (5H, m, aromatic), 7.6—7.8

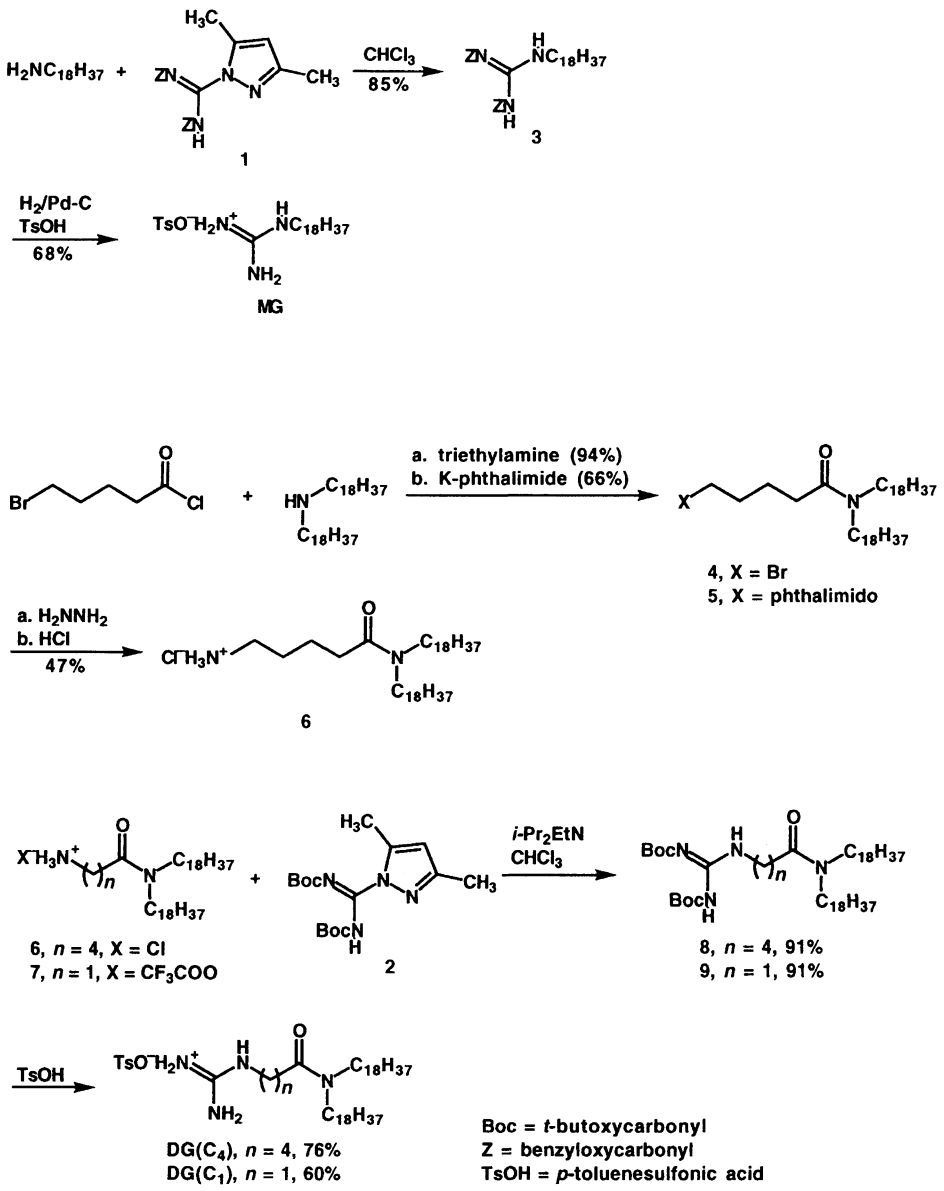

Chart 2.

(1H, br, NH), 8.9—9.1 (1H, br, NH). Found: C, 61.86; H, 5.94; N, 20.56%. Calcd for $C_{14}H_{16}N_4O_2$: C, 61.75; H, 5.92; N, 20.57%.

3,5-Dimethylpyrazole-1-[*N*,*N*′-bis(benzyloxycarbonyl)]carboxamidine (1). To a suspension of NaH (washed with hexane and dried, 377 mg, 16.4 mmol) in THF (20 mL) was added 3,5-dimethylpyrazole-1-(*N*-benzyloxycarbonyl)carboxamidine (1.27 g, 4.68 mmol) at 0 °C. After being stirred at 0 °C for 10 min, *N*-(benzyloxycarbonyloxy)succinimide (1.75 g, 7.02 mmol) was added. The whole mixture was stirred at room temperature for 17 h, followed by dilution with ethyl acetate. This was washed with water and brine, dried over Na_2SO_4, and concentrated to give a brown oil. This oil was chromatographed on SiO_2 (100 g, 6 : 1, 4 : 1, and then 3 : 1 hexane/ethyl acetate) to give **1** (1.36 g, 71%) as colorless oil. TLC R_f 0.23 (4 : 1 hexane/ethyl acetate); ^{1}H NMR ($CDCl_3$) δ = 2.19 (3H, s, CH_3), 2.55 (3H, s, CH_3), 5.21 (4H, s, 2 CH_2O), 5.98 (1H, s, vinyl), 7.3—7.5 (10H, m, aromatic), 9.4—9.6 (1H, br, NH); HRMS (FAB) *m/z* Calcd for $C_{22}H_{23}N_4O_4$: [(M + H)$^+$], 407.1719. Found: *m/z* 407.1717. Found: C, 64.71; H, 5.48; N, 13.34%. Calcd for $C_{22}H_{22}N_4O_4 \cdot 1/5H_2O$: C, 64.44; H, 5.51; N, 13.66%.

3,5-Dimethylpyrazole-1-[*N*,*N*′-bis(*t*-butoxycarbonyl)]carboxamidine (2). To a suspension of powdered LiH (513 mg, 64.5 mmol) in THF (40 mL) 3,5-dimethylpyrazole-1-carboxamidine nitrate (3.24 g, 16.1 mmol) and di-*t*-butyl dicarbonate (10.56 g, 48.4 mmol) were added. The resulting mixture was refluxed for 3 h. Water was slowly added at 0 °C and THF was removed by evaporation. The residual aqueous layer was extracted with CH_2Cl_2. The combined extracts were dried over Na_2SO_4 and concentrated. The residue was recrystallized from hexane at −20 °C to give **2** (4.26 g, 78%) as a colorless powder. Mp 97.2—99.0 °C; TLC R_f 0.69 (2 : 1 hexane/ethyl acetate); ^{1}H NMR ($CDCl_3$) δ = 1.50 (9H, s, *t*-C_4H_9), 1.54 (9H, s, *t*-C_4H_9), 2.21 (3H, s, CH_3), 2.55 (3H, s, CH_3), 5.95 (1H, s, vinyl), 9.04 (1H, s, 1, NH). Anal. Found: C, 56.77; H, 7.74; N, 16.56%. Calcd for $C_{16}H_{26}N_4O_4$: C, 56.79; H, 7.74; N, 16.56%.

1,2-Bis(benzyloxycarbonyl)-3-octadecylguanidine (3). A mixture of **1** (627 mg, 1.54 mmol) and octadecylamine (416 mg, 1.54 mmol) in $CHCl_3$ (2 mL) was allowed to stand at room temperature for 3 h followed by removal of the solvent under reduced

pressure. The resulting residue was chromatographed on SiO_2 (60 g, 6 : 1 hexane/ethyl acetate) to give **3** (761 mg, 85%) as a colorless wax. TLC R_f 0.81 (2 : 1 hexane/ethyl acetate); ^{1}H NMR ($CDCl_3$) δ = 0.88 (3H, t, J = 6.7 Hz, CH_3), 1.2—1.4 (30H, m, 15 CH_2), 1.5—1.7 (2H, m, CH_2CH_2N), 3.41 (2H, dt, J = 7.2, 7.2 Hz, CH_2N), 5.13 (2H, s, CH_2O), 5.18 (2H, s, CH_2O), 7.2—7.5 (10H, m, aromatic), 8.29 (1H, br s, NH), 11.75 (1H, s, NH). Found: C, 72.65; H, 9.29; N, 7.25%. Calcd for $C_{35}H_{53}N_3O_4$: C, 72.50; H, 9.21; N, 7.25%.

1-Octadecylguanidinium *p*-Toluenesulfonate (MG). A mixture of **3** (761 mg, 1.31 mmol), TsOH (226 mg, 1.31 mmol), and Pd/charcoal (76 mg) in CH_3OH (4 mL) was stirred at room temperature under hydrogen for 3.5 h. Pd/charcoal was removed by filtration through a Celite pad, and the filtrate was kept at −20 °C to give a solid, which was collected, washed with CH_3OH, and dried to give MG (433 mg, 68%). Mp 120.0—120.5 °C; ^{1}H NMR (DMSO-d_6,) δ = 0.85 (3H, t, J = 6.6 Hz, CH_3), 1.1—1.5 (32H, m, 16 CH_2), 2.29 (3H, s, $PhCH_3$), 3.06 (2H, t, J = 7.0 Hz, CH_2N), 6.7—7.3 (5H, br, 2 NH_2 and NH), 7.12 (2H, d, J = 7.9 Hz, aromatic), 7.48 (2H, d, J = 7.9 Hz, aromatic). Found: C, 64.54; H, 10.21; N, 8.51%. Calcd for $C_{26}H_{49}N_3O_3S$: C, 64.56; H,10.21; N, 8.69%.

5-Bromo-*N*,*N*-dioctadecylpentanoylamide (4). To a solution of dioctadecylamine[17] (5.06 g, 9.71 mmol) and triethylamine (2.70 mL, 19.4 mmol) in CH_2Cl_2 (300 mL) was added a solution of 5-bromovaleryl chloride (2.60 mL, 2.11 mmol) in CH_2Cl_2 (30 mL). The resulting mixture was stirred for 2 h at room temperature. This was washed with satd. aqueous Na_2CO_3 (×2) and water (×5), and then dried over Na_2SO_4. Removal of the solvent under reduced pressure gave an oil. After this was dissolved in hexane (200 mL), an insoluble material was removed, and the filtrate was concentrated to give **4** (6.25 g, 94%) as a yellow wax. The product was pure enough to use for the following reaction. An analytically pure product was obtained after chromatography on SiO_2 (8 : 1, 6 : 1, and then 4 : 1 hexane/ethyl acetate). TLC R_f 0.51 (4 : 1 hexane/ethyl acetate); ^{1}H NMR ($CDCl_3$) δ = 0.84 (6H, t, J = 6.7 Hz, 2 CH_3), 1.2—1.4 (60H, m, 30 CH_2 in C_{18} chains), 1.4—1.6 (4H, m, 2 CH_2CH_2N), 1.7—1.8 (2H, m, CH_2), 1.8—2.0 (2H, m, CH_2), 2.31 (2H, t, J = 7.1 Hz, $CH_2C(O)$), 3.19 (2H, t, J = 7.6 Hz, CH_2N), 3.27 (2H, t, J = 7.6 Hz, CH_2N), 3.42 (2H, t, J = 6.6 Hz, CH_2Br). Found: C, 72.21; H, 12.15; N, 2.08%. Calcd for $C_{41}H_{82}BrNO$: C, 71.89; H, 12.07; N, 2.04%.

5-Phthalimido-*N*,*N*-dioctadecylpentanoylamide (5). A mixture of **4** (6.25 g, 9.14 mmol) and potassium phthalimide (3.64 g, 19.68 mmol) in DMF (100 mL) was stirred at 85 °C for 22 h. The solvent was removed under a vacuum and the residue was dissolved in CH_2Cl_2. The resulting solution was washed with satd. aqueous Na_2CO_3 (×2) and water (×3), and then dried over Na_2SO_4. After evaporation of the solvent, the residue was chromatographed on SiO_2 (200 g, 5 : 1 hexane/ethyl acetate) to give **5** (4.51 g, 66%) as a colorless wax. TLC R_f 0.30 (4 : 1 hexane/ethyl acetate); ^{1}H NMR ($CDCl_3$) δ = 0.86 (6H, t, J = 6.6 Hz, 2 CH_3), 1.1—1.4 (60H, m, 30 CH_2 in C_{18} chains), 1.4—1.6 (4H, m, 2 CH_2CH_2N), 1.6—1.8 (4H, m, 2 CH_2), 2.32 (2H, t, J = 6.9 Hz, $CH_2C(O)$), 3.18 (2H, t, J = 7.7 Hz, CH_2N), 3.25 (2H, t, J = 7.6 Hz, CH_2N), 3.70 (2H, t, J = 6.6 Hz, CH_2N), 7.66—7.71 (2H, m, aromatic), 7.79—7.84 (2H, m, aromatic). Found: C, 78.35; H, 11.54; N, 3.71%. Calcd for $C_{49}H_{86}N_2O_3$: C, 78.34; H, 11.54; N, 3.73%.

4-(Dioctadecylcarbamoyl)butylammonium Chloride (6). A mixture of **5** (4.29 g, 5.73 mmol) and hydrazine hydrate (3.0 mL, 62.0 mmol) in C_2H_5OH (150 mL) was refluxed for 12 h. After being cooled to room temperature, conc. hydrochloric acid (15 mL) was added and the resulting mixture was stirred for 1 h. An insoluble material was removed by filtration and the filtrate was concentrated to dryness. The residue was crystallized from ethyl acetate (70 mL) to give **6** (1.76 g, 47%) as a colorless powder. Mp 72.2—72.9 °C; ^{1}H NMR ($CDCl_3$) δ = 0.88 (6H, t, J = 6.7 Hz, 2 CH_3), 1.1—1.4 (60H, m, 30 CH_2 in C_{18} chains), 1.4—1.6 (4H, m, 2 CH_2CH_2N), 1.7—1.9 (4H, m, 2 CH_2), 2.37 (2H, t, J = 6.3 Hz, $CH_2C(O)$), 3.0—3.1 (2H, m, CH_2NH_3), 3.18 (2H, t, J = 7.7 Hz, CH_2N), 3.25 (2H, t, J = 7.5 Hz, CH_2N), 8.50 (3H, br s, NH_3). Found: C, 74.85; H, 13.01; N, 4.25%. Calcd for $C_{41}H_{85}ClN_2O$: C, 74.89; H, 13.03; N, 4.26%.

5-[2,3-Bis(*t*-butoxycarbonyl)guanidino]-*N*,*N*-dioctadecylpentanamide (8). A solution of **2** (247 mg, 0.73 mmol), **6** (576 mg, 0.88 mmol), and (*iso*-$C_3H_7)_2C_2H_5N$ (114 mg, 0.88 mmol) in $CHCl_3$ (10 mL) was stirred at 30—35 °C for 12 h. This was concentrated under reduced pressure and the residue was chromatographed on SiO_2 (30 g, 5 : 1 hexane/ethyl acetate) to give **8** (571 mg, 91%) as colorless wax. TLC R_f 0.65 (2 : 1 hexane/ethyl acetate); ^{1}H NMR ($CDCl_3$) δ = 0.87 (6H, t, J = 6.8 Hz, 2 CH_3), 1.2—1.8 (86H, m, 34 CH_2 in C_{18} chains, 2 CH_2, and 2 t-C_4H_9), 2.30 (2H, t, J = 7.1 Hz, $CH_2C(O)$), 3.18 (2H, t, J = 7.7 Hz, CH_2N), 3.27 (2H, t, J = 7.7 Hz, CH_2N), 3.43 (2H, dt, J = 6.2 Hz, CH_2NH), 8.33 (1H, br s, NH), 11.49 (1H, s, NH). Found: C, 72.38; H, 11.96; N, 6.48%. Calcd for $C_{52}H_{102}N_4O_5$: C, 72.34; H, 11.91; N, 6.49%.

1-[4-(Dioctadecylcarbamoyl)butyl]guanidinium *p*-Toluenesulfonate (DG(C_4)). A solution of **8** (350 mg, 0.41 mmol) and $TsOH\cdot H_2O$ (925 mg, 4.86 mmol) in THF (1 mL) was stirred at room temperature for 24 h. This was diluted with $CHCl_3$ (5 mL) and washed with water (5 mL×5) and brine. The organic layer was dried over Na_2SO_4 and concentrated to give an oil, which was recrystallized twice from THF–CH_3CN (1 : 1) at 4 °C to give DG(C_4) (258 mg, 76%) as colorless powder. Mp 43.3—45.3 °C; ^{1}H NMR ($CDCl_3$) δ = 0.88 (6H, t, J = 6.7 Hz, 2 CH_3), 1.2—1.8 (64H, m, 32 CH_2 in C_{18} chains), 2.30 (2H, br s, $CH_2C(O)$), 2.35 (3H, s, $ArCH_3$), 3.1—3.3 (6H, m, 2 CH_2N and CH_2NH), 6.9—7.1 (4H, br 2 NH_2), 7.17 (2H, d, J = 8.0 Hz, aromatic), 7.65 (1H, br s, NH), 7.73 (2H, d, J = 8 Hz, aromatic). Found: C, 70.20; H, 11.40; N, 6.70%. Calcd for $C_{49}H_{94}N_4O_4S$: C, 70.45; H, 11.34; N, 6.71%.

(Dioctadecylcarbamoyl)methylammonium Chloride. This compound was prepared in a manner similar to that described for its ditetradecyl derivative[18] from dioctadecylamine[17] and chloroacetyl chloride via a phthalimide. Colorless powder. Mp 70—111 °C (LC phase); ^{1}H NMR ($CDCl_3$) δ = 0.88 (6H, t, J = 6.7 Hz, 2 CH_3), 1.1—1.4 (60H, m, 30 CH_2 in C_{18} chains), 1.4—1.6 (4H, m, 2 CH_2CH_2N), 3.15 (2H, t, J = 7.7 Hz, CH_2N), 3.29 (2H, t, J = 7.6 Hz, CH_2N), 3.96 (2H, s, $NCH_2C(O)$). Found: C, 73.72; H, 12.84; N, 4.60%. Calcd for $C_{38}H_{79}ClN_2O\cdot 1/5H_2O$: C, 73.72; H, 12.93; N, 4.52%.

(Dioctadecylcarbamoyl)methylammonium Trifluoroacetate (7). A solution of (dioctadecylcarbamoyl)methylammonium chloride (640 mg, 1.04 mmol) in $CHCl_3$ (20 mL) was washed successively with 1 M NaOH, water, and brine. After drying over Na_2SO_4, trifluoroacetic acid (0.5 mL, 6.50 mmol) was added to the solution. A volatile material was removed by evaporation and the residue was recrystallized from ether/CH_3CN to give **7** (668 mg, 93%) as colorless crystals. Mp 61.3—61.8 °C; ^{1}H NMR ($CDCl_3$) δ = 0.88 (6H, t, J = 6.6 Hz, 2 CH_3), 1.1—1.6 (64H, m, 32 CH_2 in C_{18} chains), 3.16 (2H, t, J = 7.6 Hz, CH_2N), 3.32 (2H, t, J = 7.6 Hz, CH_2N), 3.99 (2H, br s, $CH_2C(O)$), 7.77 (3H, br s, NH_3). Found: C, 69.36; H, 11.52; N, 4.02%. Calcd for $C_{40}H_{79}F_3N_2O_3$: C, 69.32; H, 11.49; N, 4.04%.

2-[2, 3-Bis(*t*-butoxycarbonyl)guanidino]-*N*, *N*-dioctadecylacetamide (9). A solution of **2** (76 mg, 0.22 mmol), **7** (173 mg, 0.25 mmol), and (*iso*-$C_3H_7)_2C_2H_5N$ (65 mg, 0.50 mmol) in $CHCl_3$

(1.5 mL) was stirred at 30 °C for 3 d. After this was concentrated under reduced pressure, the residue was chromatographed on SiO_2 (20 g, 15 : 1 and then 6 : 1 hexane/ethyl acetate) to give **9** (164 mg, 91%) as colorless powder. Mp 71.8—72.8 °C; TLC R_f 0.58 (4 : 1 hexane/ethyl acetate); ^{1}H NMR ($CDCl_3$) δ = 0.88 (6H, t, J = 6.7 Hz, 2 CH_3), 1.1—1.4 (60H, m, 30 CH_2 in C_{18} chains), 1.4—1.6 (4H, m, 2 CH_2CH_2N), 1.50 (9H, s, t-C_4H_9), 1.51 (9H, s, t-C_4H_9), 3.16 (2H, t, J = 7.7 Hz, CH_2N), 3.33 (2H, t, J = 7.7 Hz, CH_2N), 4.19 (2H, d, J = 3.9 Hz, $NCH_2C(O)$), 9.47. (1H, br s, NH), 11.42 (1H, s, NH). Found: C, 71.67; H, 11.78; N, 6.67%. Calcd for $C_{49}H_{96}N_4O_5$: C, 71.66; H, 11.78; N, 6.82%.

[(Dioctadecyl)carbamoylmethyl]guanidinium *p*-Toluenesulfonate (DG(C_1)). A solution of **9** (210 mg, 0.26 mmol) and TsOH·H_2O (528 mg, 3.07 mmol) in THF (1 mL) was stirred at room temperature for 24 h. This was diluted with $CHCl_3$ (5 mL) and washed with water and brine. The organic layer was dried over Na_2SO_4 and concentrated to give an oil, which was recrystallized from THF/CH_3CN (1 : 1) at 4 °C to give DG(C_1) (123 mg, 60%) as colorless powder. Mp 68.0—70.0 °C; ^{1}H NMR ($CDCl_3$) δ = 0.88 (6H, t, J = 6.6 Hz, 2 CH_3), 1.1—1.6 (64H, m, 32 CH_2 in C_{18} chains), 2.35 (3H, s, $PhCH_3$), 3.12 (2H, t, J = 7.3 Hz, CH_2N), 3.22 (2H, t, J = 7.8 Hz, CH_2N), 4.07 (2H, d, J = 4.5 Hz, $NCH_2C(O)$), 7.16 (2H, d, J = 8.1 Hz, Ar), 7.2—7.4 (4H, br, 2 NH_2), 7.55 (1H, br s, NH), 7.72 (2H, d, J = 8.1 Hz, Ar). Found: C, 69.62; H, 11.13; N, 7.05%. Calcd for $C_{46}H_{88}N_4O_4S$: C, 69.65; H, 11.18; N, 7.06%.

***π*–*A* Isotherm Measurement and LB Transfer.** *π*–*A* Isotherms were measured with a computer-controlled film balance system FSD-50 (USI System, Fukuoka). The concentration of polycarboxylates in the subphase was 0.1 mM. An equivalent amount of NaOH was added to the subphase in order to convert carboxylic acid to carboxylate. A mixture of benzene/ethanol (80/20) was used as a spreading solvent. Compression was started about 10 min after spreading at a rate of 0.2 mm s^{-1} (or 20 mm^2 s^{-1} based on area). The subphase temperature was kept at 20±0.2°C. The surface pressures were measured by a Wilhelmy plate, which was calibrated with the transition pressure of an octadecanoic acid monolayer.

LB films were transferred onto gold-deposited glass plates for reflection-absorption FT-IR spectroscopy. The substrate was prepared as follows. A slide glass (pre-cleaned, 176×26×1 mm, Iwaki Glass) was immersed in a detergent solution overnight (Dsn 90, Bokusui Brown Co.). The glass was washed with a large excess of ion-exchanged water to remove the detergent completely, and subjected to sonication in fresh ion-exchanged water several times. After the glass was dried under a vacuum for over 1 h, thin layers of chromium and gold were consecutively formed by the vapor-deposition method (1000 Å Au/50 Å Cr/slide glass) with a vapor-deposition apparatus VPC-260 (ULVAC Kyushu).

LB transfer was carried out with a FSD-21 instrument (USI System, Fukuoka) by the vertical dipping method. Monolayers were transferred on Au-coated glass plates at 30 mN m^{-1} with dipping speeds of 100 mm min^{-1} (down stroke) and 20 mm min^{-1} (up stroke). Transfer ratios were almost unity and the type of transfer was Y. When the transferred films were returned to water in the subsequent down-stroke process (usually the third transfer process), we newly prepared the film and stopped the transfer process just before the third process. Therefore, the samples used for the FT-IR measurement were always transferred under the conditions of a transfer ratio of unity. MG monolayers under certain subphase conditions were not stable against collapse and/or dissolution upon standing for a long period of time. In these cases, LB transfer was conducted once or twice immediately after the surface pressure reached 30 mN m^{-1}.

Characterization of LB Films. The FT-IR spectra (reflection-absorption spectrum (RAS) mode) were measured with LB films transferred on gold-deposited glass plates with a Nicolet 710 FT-IR spectrometer.

X-Ray photoelectron spectra (XPS) were measured for the LB films on Au/Cr/glass with Perkin–Elmer PHI 5300 ESCA. The X-Ray source was Mg $K\alpha$ (300 W). Repeated scans over the same surface region at a take off angle of 45° gave reproducible spectra. The elemental composition was obtained by dividing the observed peak area by intrinsic sensitivity factor of each element.

Molecular Model Calculation. Molecular conformations of some dicarboxylates were estimated by a Chem 3D Plus calculation based on the MM2 force field (ver. 3.1.2, Cambridge Scientific Computing). The structural error was minimized in bond length, bond angle, planar atom flattening, and double rotation terms (minimum RMS error, 0.001; minimum RMS gradient, 0.001); then, the conformational energy was optimized (minimum RMS gradient, 0.001). The MM2 parameters given in the program were used without any modification. Several stable conformers were obtained depending on the initial conditions. Since lipid molecules in a monolayer tend to form condensed phases at high pressures to achieve a large van der Waals interaction between chains, the final selection among the candidates was done by taking into account the packing of bound lipids. We used the following conformers as the most appropriate ones: The distance between two carboxylate groups within a molecule is small, and, if several conformers have similar carboxylate distances, their parallel orientation is more favored.

Results and Discussion

Syntheses of Guanidinium Amphiphiles. Acylated pyrazole-1-carboxamidine hydrochloride has recently been reported as being an efficient guanylating agent.[19] Although these agents have several advantages over conventional guanylating agents, such as *O*-methylisourea hydrogensulfate or *S*-methylisothiourea sulfate, pyrazole-1-carboxamidine hydrochloride needs to be synthesized.[20] In this study we developed analogous agents, **1** and **2**, for the preparation of guanidinium amphiphiles. They were readily synthesized by the acylation of commercial 3,5-dimethylpyrazole-1-carboxyamidine nitrate, and gave satisfactory yields in guanylation of amine. By using **1**, 1-octadecylguanidinium *p*-toluenesulfonate (MG) was easily prepared. Thus, octadecylamine was allowed to react with **1** to give bis Z-protected guanidine **3**. Deblocking of the Z group by hydrogenolysis in the presence of an equimolar amount of *p*-toluenesulfonic acid (TsOH) gave MG. Z-Protected **1** was used to avoid a loss of the product during an aqueous workup of the deprotection procedure. The bis Boc derivative **2** was used for the preparing DG(C_1) and DG(C_4). Thus, amine salts **6** or **7** were prepared by the acylation of dioctadecylamine, followed by a Gabriel synthesis (the trifluoroacetate **7** was used because its hydrochloride was hygroscopic). Their guanylation by **2** in the presence of *N*,*N*-diisopropylethylamine gave the corresponding bis Boc-protected guanidines, **8** and **9**. Deblocking of Boc groups was done with excess TsOH.

Amphiphile Structure and Effect of Aqueous Linear Dicarboxylates. *π*–*A* Isotherms of MG, DG(C_1), and

$DG(C_4)$ monolayers on pure water are shown in Fig. 1. The isotherm of MG on pure water displayed a poor reproducibility among several trials. The molecular area at high surface pressures is smaller than the cross-sectional area of a single alkyl chain (0.2 nm^2),[21] implying that part of the monolayer is dissolved in the subphase upon compression. In fact, the surface area of MG gradually decreases when the monolayer is kept at 30 $mN\,m^{-1}$. In contrast, $DG(C_1)$ and $DG(C_4)$ gave completely overlapping isotherms upon separate measurements, and showed a high monolayer stability even at high pressures. These isotherms give condensed phases with limiting areas of 0.45 and 0.49 nm^2 for $DG(C_1)$ and $DG(C_4)$, respectively, that are comparable to the cross-sectional area of dialkyl chain (0.4 nm^2). Therefore, these monolayers form well-packed condensed phases.

π–A Isotherms of these three monolayers were measured on 0.1 mM aqueous solutions of linear dicarboxylates. Equivalent amounts of NaOH were added to the subphase in order to convert carboxylic acid to carboxylates; also the guanidine group is known to be in its ionized form[22] under the experimental condition (subphase pH is ca. 6). The results are summarized in Fig. 2. All of the isotherms showed satisfactory reproducibility. It is clear that MG monolayer is greately stabilized in the presence of dicarboxylates. The stabilization of the MG monolayer was also observed in the presence of FAD having two phosphate groups.[12]

The shapes of these π–A isotherms are affected by the kind of dicarboxylates. The influence was most pronounced in the case of a MG monolayer (Fig. 2A). The oxalate ion induced a highly condensed isotherm, with its limiting area being relatively close to the cross-sectional area of a single alkyl chain. The molecular area increased as the number of spacer methylenes in the dicarboxylate increased from oxalate to adipate. This suggests that specific binding between guanidinium and carboxylate is favored at the interface, and it affects the molecular packing in the monolayer. Although a similar behavior was observed for $DG(C_1)$ and $DG(C_4)$ monolayers (Figs. 2B and 2C, respectively), the influence of

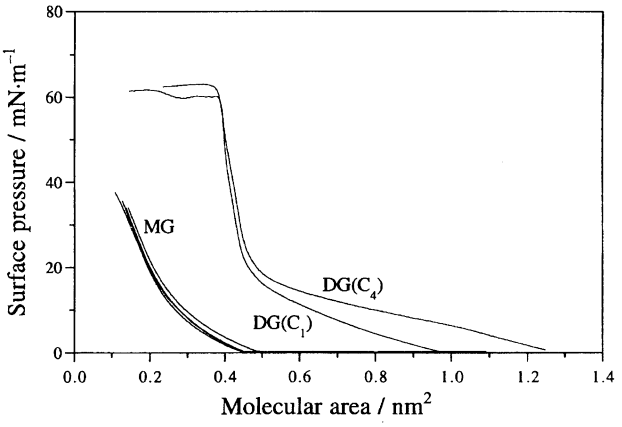

Fig. 1. π–A Isotherms of guanidinium monolayers (MG, $DG(C_1)$, and $DG(C_4)$) on pure water at 20.0±0.2°C. Four isotherms of MG monolayer in separate measurements are shown to represent a poor reproducibility.

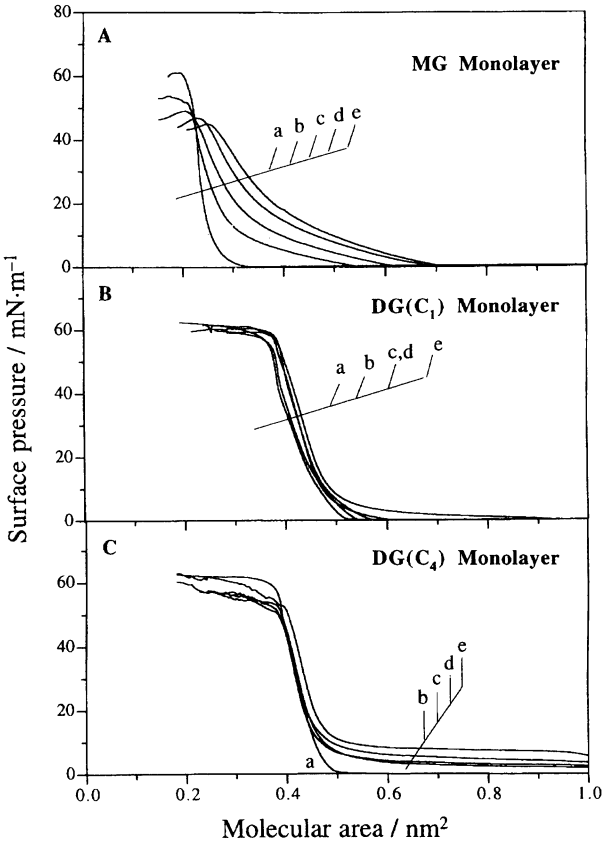

Fig. 2. π–A Isotherms of monoalkyl and dialkyl guanidinium monolayers on 0.1 mM aqueous dicarboxylates at 20.0±0.2°C; a: oxalate, b: malonate, c: succinate, d: glutarate, e: adipate).

dicarboxylates was lessened, because the latter double-chain guanidiniums can form condensed monolayers. even on pure water.

For a quantitative evaluation of these effects, we compared the molecular areas at 30 $mN\,m^{-1}$. The areas were normalized with respect to those observed with oxalate to cancel the difference in the intrinsic molecular area. The normalized areas are plotted as a function of the length of the methylene chain (n) in Fig. 3. Since the standard errors of all the plots in repeated measurements were less than 0.004, the changes in the relative area of Fig. 3 are significant enough. The MG monolayer showed the largest dependency on the methylene length, as expected from Fig. 2. For example, the area on adipate was almost 1.4-times as large as that on oxalate. The relative molecular area increased almost linearly as the methylene chain was extended.

Both of the dialkyl guanidinium monolayers showed a smaller dependency on the methylene length than that observed on the MG monolayer. The difference in the normalized area was within 10% from $n=1$ to 4 (Fig. 3). The greater packing ability of dialkyl compounds in monolayers would prevent the monolayers from any further expansion. Morphology analyses of the monolayers by electron diffraction revealed that DPPC with two C_{16} chains has an aggregation ability comparable to sodium arachidate with a longer C_{20}-

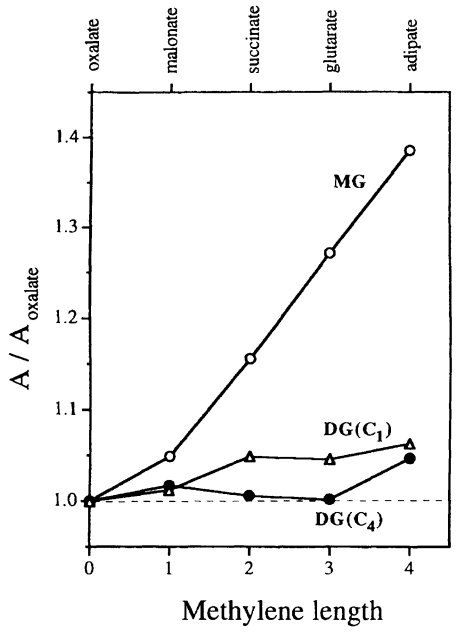

Fig. 3. Influence of the methylene length (n) in linear dicarboxylates on the relative molecular area of guanidinium monolayers at 30 mN m^{-1} and 20.0±0.2 °C. The plotted molecular areas are normalized relative to that of observed in the presence of oxalate (see text).

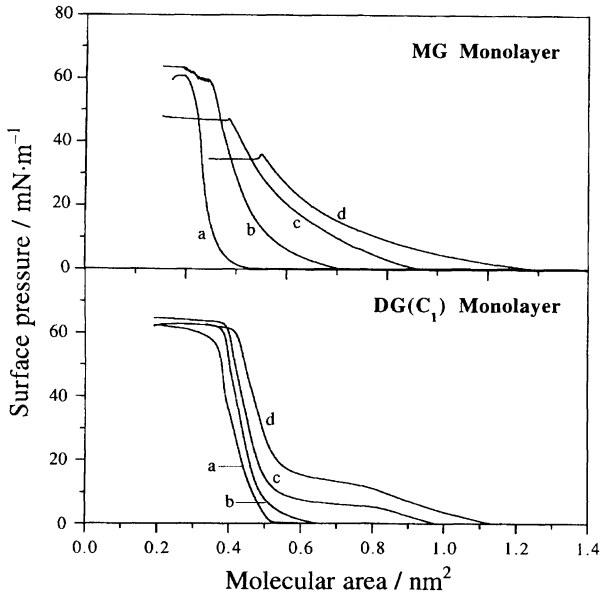

Fig. 4. π–A Isotherms of guanidinium monolayers on 0.1 mM aqueous dicarboxylates, a: oxalate, b: phthalate, c: *cis*-1,2-cyclohexanedicarboxylate, d: 1,1-cyclohexanediacetate, at 20.0±0.2°C.

monoalkyl chain.[23] The DG(C_1) monolayer on mica transferred from pure water was stable enough to give a molecular image in an AFM observation, even in its amorphous state,[24] while the MG monolayer alone was not stable enough.[13] The cohesive force among alkyl chains is greater in monolayers of dialkyl amphiphiles than in monolayers of monoalkyl amphiphiles.

An interesting difference was observed between the two dialkyl monolayers. The molecular area of the DG(C_4) monolayer hardly changed, except for adipate, while the area of DG(C_1) gradually increased as the methylene length between the carboxylate groups increased. When long alkyl chains are connected closely to the guanidinium polar site, their packing would be readily affected by the changing nature of the head group due to carboxylate binding. In the case of the DG(C_4) monolayer, the C_4 spacer between the alkyl chain and the guanidinium head group appears to moderate the influence of the dicarboxylate binding at the head group. The monolayer of DG(C_1) was better suited in the present study, since it is affected more strongly by aqueous dicarboxylate. Thus, DG(C_1) was used as dialkyl guanidinium monolayer in subsequent experiments.

Other Polycarboxylates and Monolayer Behavior. The effects of other polycarboxylates (see Chart 1) on the monolayer behavior of MG and DG(C_1) were subsequently investigated. Figure 4 compares the π–A isotherms MG and DG(C_1) in the presence of four dicarboxylates as examples: oxalate, phthalate, *cis*-1,2-cyclohexanedicarboxylate, and 1,1-cyclohexanediacetate. Oxalate is the smallest dicarboxylate. Phthalate has a benzene ring and *cis*-1,2-cyclohexanedicarboxylate and 1,1-cyclohexanediacetate have a cyclohexane backbone. The latter three dicarboxylates have close molecular sizes with a different relative orientation of the two carboxylate groups. The MG monolayer again underwent greater changes than did the DG(C_1) monolayers, though the pattern of the changes was identical. The molecular area increased in both cases in the order oxalate < phthalate <*cis*-1,2-cyclohexanedicarboxylate < 1,1-cyclohexanediacetate. Oxalate and phthalate gave condensed monolayers, while more expanded monolayers were formed with the latter two dicarboxylates.

The effects of all of the polycarboxylates used in this study are compared in Fig. 5 by using the relative molecular area at 30 mN m^{-1}. A greater expansion was generally observed in the case of the MG monolayer, and the effect of individual polycarboxylates was similar for both monolayers, though some polycarboxylates, such as Kemp's triacid showed exceptional behavior. The observed effects can be summarized as follows: i) In the case of simple aliphatic dicarboxylates (group 1), the molecular areas increased as the number of the spacer methylene increased. ii) Polycarboxylates with the cyclohexane skeleton (group 3) gave larger molecular areas than did the other polycarboxylates. Especially, Kemp's triacid and 1,1-cyclohexanediacetate displayed a greater expansion. iii) Polycarboxylates with unsaturated bonds (groups 2 and 4) showed smaller effects than did the corresponding saturated polycarboxylates (groups 1 and 3, respectively). iv) Among similar types of polycarboxylates, the area expansion was lessened as the number of the carboxylate groups in a molecule increased.

All of these data indicate the importance of the number and relative disposition of carboxylate units in a polycarboxylate molecule in modifying the molecular packing of guanidinium monolayers.

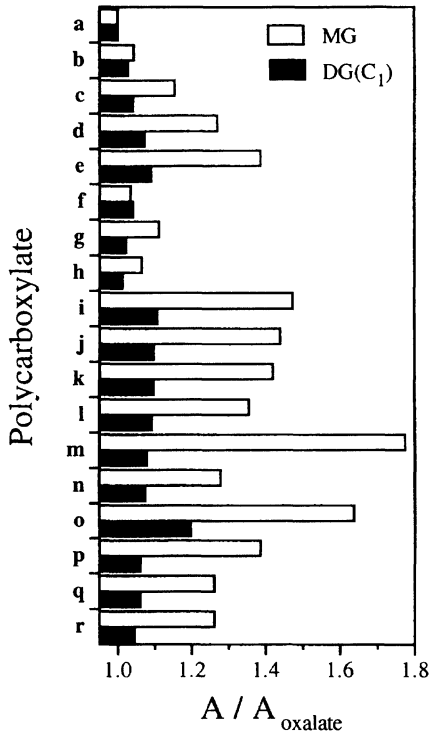

Fig. 5. Relative molecular area of guanidinium monolayers at 30 mN m^{-1} on aqueous polycarboxylates (open rectangle: MG, filled rectangle: DG(C_1)); a: oxalate (standard), b: malonate, c: succinate, d: glutarate, e: adipate, f: fumarate, g: maleate, h: *trans*-aconitate, i: *cis*-1,2-cyclohexanedicarboxylate, j: *trans*-1,2-cyclohexanedicarboxylate, k: *trans*-1,4-cyclohexanedicarboxylate, l: r-1,c-3,c-5-cyclohexanetricarboxylate, m: Kemp's acid, n: all *cis*-cyclohexanehexacarboxylate, o: 1,1-cyclohexanediacetate, p: *trans*-1,2-diaminocyclohexane-*N*,*N*,*N*′,*N*′-tetraacetate, q: phthalate, r: trimesate. The molecular areas are normalized by the area observed in the presence of oxalate. The standard error of repeated measurements was within 0.005.

XPS Analyses of Guanidinium/Carboxylate Complexes. In order to obtain additional information concerning the guanidinium/carboxylate binding, the transferred LB films on gold-deposited glass plates were characterized by an XPS analysis. An XPS measurement of oriented samples, such as LB films, sometimes needs depth correction, because elements near to the outermost surface give stronger signals than those from elements deeper in the sample.[25] Fortunately, oxygen and nitrogen atoms, which we use for determining the host/guest ratio, are located close in the film, and a structural correction is not required. The DG(C_1) molecule without a counter ion possesses one oxygen and four nitrogen atoms (O/N = 1/4 = 0.25), and a 1 : 1 guanidinium/COO^- complex gives a ratio of 0.75 (O/N = 3/4). If one carboxylate group in dicarboxylate binds to DG(C_1) and the other carboxylate group remains unbound (guanidinium/$(COO^-)_2$ complex), the O/N ratio would be 5/4 = 1.25. Similarly, although MG in guanidinium/COO^- complex has an O/N ratio of 0.67 (2/3), the guanidinium/$(COO^-)_2$ complex of MG gives O/N = 4/3 = 1.33. If the monolayer keeps *p*-toluenesulfonate as a counter ion, one can detect sulfur.

The XPS results of the films are summarized in Table 1. Sodium and sulfur were not detected in these films, except for a 0.03% S content in DG(C_1) film transferred from pure water. *p*-Toluenesulfonate must be replaced by OH^- almost completely. In fact, the observed O/N value of the film transferred from the water subphase is close to 0.5 of DG(C_1) with an OH^- counter ion. The other DG(C_1) films with various templates shows O/N values of 0.75±0.05 with a calculated COO^-/lipid ratios of 0.8—1.1, except for the case of malonate. This result confirms that the carboxylate group and the guanidinium group essentially form a 1 : 1 complex in all of the DG(C_1) films. A similar tendency was observed in MG films. The O/N values of the MG film are somewhat smaller than 0.67 of the stoichiometric complex with calculated COO^-/lipid values of 0.6—0.7. The binding of guanidinium/carboxylate at the interface is expected to be quite efficient, because a quite high binding constant was observed for the guanidinium/phosphate system at the interface,[6] and the affinity of guanidinium/carboxylate is comparable to that of guanidinium/phosphate.[14] Therefore, the binding stoichiometry of less than unity observed for DG/malonate and MG/dicarboxylate pairs may come from intrinsic reasons, rather than simple unsaturation. Among the linear dicarboxylates of Table 1, the binding motif of oxalate is unique, as discussed below. However, the others are commonly bound as guanidinium/carboxylate pairs, and the ratio is smallest with malonate and increases with increasing methylene spacers. Shorter dicarboxylates, except for oxalate (e.g., malonate), may not occupy the whole guanidinium site at the interface due to a steric restriction. This factor would be more pronounced in the case of the MG monolayer, because the guanidinium function is more densely aligned at the interface, leading to less than stoichiometric carboxylate binding.

FT-IR Investigation on Guanidinium/Carboxylate Complexes. The FT-IR spectra were closely examined only in the carbonyl region of 1400—1900 cm^{-1}, because the guanidinium peaks at around 3400 cm^{-1} were too broad to be interpreted. It is reported that the $\nu_{C=O}$ peak of free COOH appears at 1700—1725 cm^{-1} and hydrogen bond formation shifts this band by as much as 30 cm^{-1} towards lower frequency.[26] The antisymmetric band of carboxylate is located at between 1550 and 1610 cm^{-1}.[26] It was also reported that the peak of the carboxylate bound to guanidinium through hydrogen bonding appears at 1633 cm^{-1} due to a large proton polarizability, and that unbound COO^- is located at 1595 cm^{-1}.[27] Therefore, the peak of hydrogen-bonded carboxylate with guanidinium may be located at around 1650 cm^{-1}, depending on the extent of proton polarizability. The $\nu_{C=O}$ peak of the secondary amide is usually found at between 1630 and 1680 cm^{-1}.[28]

The IR spectra of DG(C_1) films transferred from pure water, aqueous oxalate, and aqueous malonate are shown in Fig. 6. The film transferred from pure water shows one peak at 1653 cm^{-1}, which is assigned to amide C=O of DG(C_1), itself. This peak is present for all DG(C_1) films at between

Table 1. Elemental Composition of the Transferred LB Films as Determined by XPS Measurement[a)]

Template	C(%)	N(%)	O(%)	O/N	COO^-/lipid[b)]
DG(C_1) LB film					
None	91.30	6.01	2.66	0.443	—
Oxalate	90.76	5.20	4.04	0.777	1.08
Malonate	92.76	4.43	2.81	0.634	0.54
Suucinate	93.01	4.13	2.86	0.692	0.77
Glutarate	91.82	4.80	3.38	0.704	0.82
Adipate	93.30	3.93	2.77	0.705	0.82
trans-Aconitate	91.11	5.04	3.85	0.764	1.06
cis-1,2-Cyclohexane-Dicarboxylate	92.77	4.05	3.19	0.788	1.15
1,1-Cyclohexanediacetate	92.89	4.26	2.85	0.699	0.80
MG LB film					
Oxalate	88.62	7.44	3.94	0.530	0.59
Adipate	90.29	6.36	3.35	0.527	0.58
1,1-Cyclohexanediacetate	87.75	7.86	4.39	0.559	0.68

a) S and Na were not detected in all the films except that 0.03% of S was detected n the DG(C_1) LB film transferred from pure water. b) For the calculation of binding ratio, we assumed that unbound guanidinium possess OH^- as a counter ion. This assumption is consistent with the XPS result.

1646 and 1653 cm^{-1}. The spectrum with oxalate has two additional peaks at 1610 and 1690 cm^{-1}, which are assigned to free carboxylate (COO^-) and hydrogen-bonded carboxylate, respectively. In contrast, the spectrum with malonate shows one additional peak at 1661 cm^{-1}. It can be assigned to hydrogen-bonded carboxylate from a comparison with the reported data.

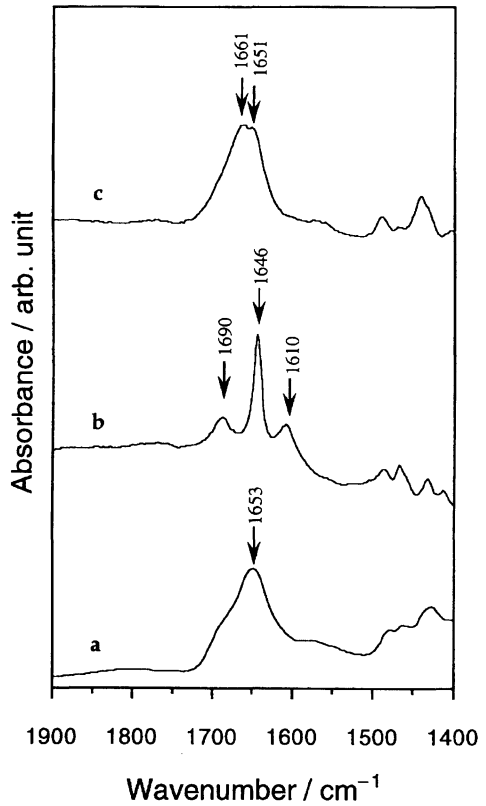

Fig. 6. FT-IR spectra (RAS mode, 1400 to 1900 cm^{-1}) of DG(C_1) LB films transferred from; a: pure water, b: 0.1 mM aqueous oxalate, c: 0.1 mM aqueous malonate.

The peak positions in this region are summarized in Table 2 for the MG and DG(C_1) monolayers. The peaks at around 1650 cm^{-1} in the DG(C_1) spectra are attributed to the amide C=O peak of the monolayer, itself. In both films, the IR spectra of the film with dicarboxylates other than oxalate give peaks of hydrogen-bonded carboxylate groups alone. Two carboxylate groups in these dicarboxylates form analogous hydrogen bonds with guanidinium lipids. In contrast, bound oxalate gives peaks of free ionized carboxylate as well as hydrogen-bonded carboxylate. Therefore, it is suggested that two carboxylate functions in oxalate bind to the monolayers through two types of pairing.

Computational Examination of Carboxylates Bound to the Guanidinium Monolayer. The XPS and FT-IR results revealed that the guanidinium function formed 1 : 1 complexes with carboxylate groups through hydrogen bonding, except for the case of oxalate. A fixed geometry

Table 2. Peak Positions in FT-IR Spectra of the Transferred LB Films in the Range of 1600 to 1700 cm^{-1}

Template	Peak positions/cm^{-1}		
DG(C_1) LB film			
None		1653	
Oxalate	1610	1646	1690
Malonate		1651	1661
trans-Aconitate		1651	1661
cis-1,2-Cyclohexanedicarboxylate		1651	1660
1,1-Cyclohexanediacetate		1655	
MG LB film			
Oxalate	1633		1684
Malonate			1668
1,1-Cyclohexanediacetate			1672

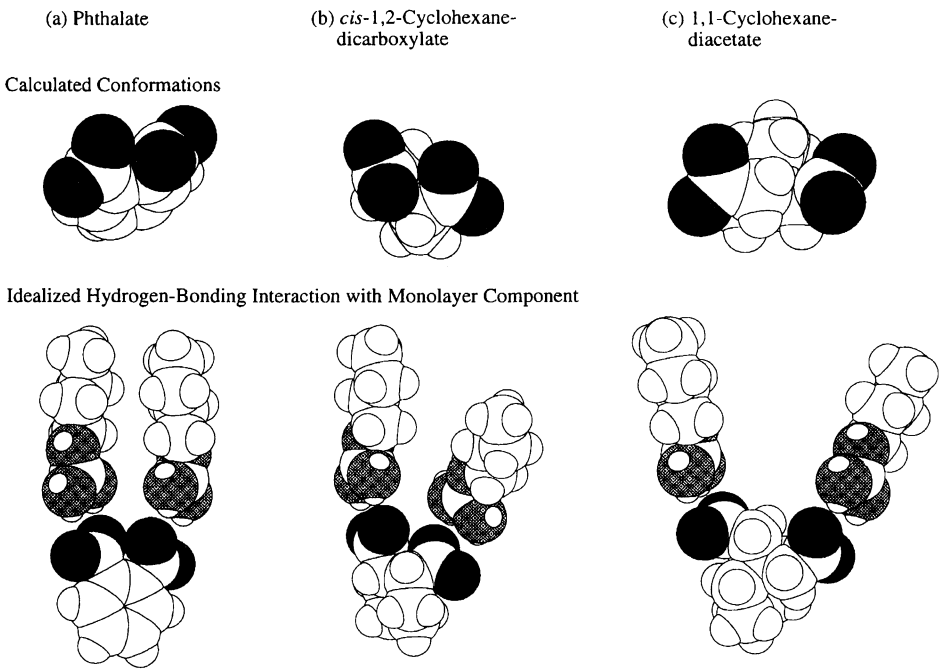

Fig. 7. Calculated conformations and idealized interaction of three dicarboxylates. Molecular conformations represented by the space-filling models were calculated with Chem 3D Plus. Oxygen atoms are shaded; a: phthalate, b: *cis*-1,2-cyclohexane-dicarboxylates, c: 1,1-cyclohexanediacetate. "Idealized Interaction" shows butylguanidinium/carboxylate complexes in which N atoms in guanidinium and O atoms in dicarboxylates are shaded. Planar binding conformation is assumed for maximized guanidinium/carboxylate interaction.

is required for effective hydrogen bond formation. Thus, relative disposition of the carboxylate groups in polycarboxylate molecules would affect the packing and arrangement of the bound guanidinium molecules. The alteration of the molecular areas in the π–A isotherm suggested that this was in fact the case.

Molecular modeling would be helpful for considering the details of a host–guest interaction. As examples, molecular conformations were examined for three templates: phthalate, *cis*-1,2-cyclohexanedicarboxylate, and 1,1-cyclohexanediacetate. These dicarboxylates possess analogous molecular sizes with different functional dispositions. The observed molecular area in the π–A isotherm increased in the order phthalate $<$*cis*-1,2-cyclohexanedicarboxylate $<$ 1,1-cyclohexanediacetate, as shown in Fig. 4. Several candidate conformers were selected for these compounds based on an MM2 calculation. A further selection was made by choosing a conformer in which the distance between two carboxylate groups is small. If several models had similar carboxylate distances, we selected a conformer which gave a parallel orientation of two carboxylate groups. These conditions were chosen because a parallel carboxylate orientation should lead to better-packed guanidinium monolayers. The conformations of the selected dicarboxylates are illustrated in Fig. 7. The distances between two carboxylate carbons are 3.03 Å for phthalate, 3.13 Å for *cis*-1,2-cyclohexanedicarboxylate, and 4.47 Å for 1,1-cyclohexanediacetate. The carboxylate groups in phthalate point in a relatively parallel direction, while two carboxylate groups are oriented far from parallel in the other cases.

These considerations are based on the premise that maximal interaction is achieved when hydrogen-bonded complexes of guanidinium and carboxylate assume planar conformations. Salunke et al.[29] and Yokomori et al.[30] discussed the possible geometries of the guanidinium/carboxylate complex, as shown in Fig. 8. They pointed out that the most probable one is the geometry shown in Fig. 8(a) on the basis of a crystallographic analysis. Models of c and d would be less stable because of the non-linear geometry of the hydrogen bonds. In the case of the interfacial interaction, guanidinium groups are exposed to water in one direction (idealized interaction model in Fig. 7), and the formation of the model in (b) is not favorable. Therefore, the hydrogen bonding pattern of Fig. 8(a) is most probable at the air–water interface as well.

The molecular packing of the guest-bound amphiphiles can be examined on the basis of the calculated dicarboxylate conformation and the 1 : 1 complex formation with a planar-binding conformation. Models of the interaction between the alkyl guanidinium and the dicarboxylate are shown in Fig. 7 as an idealized interaction model. The packing mode of the alkyl chains of the monolayers is significantly influenced by the shape of template molecules. Two carboxylate groups in phthalate are located close to each other and directed in the same way, promoting the packing of the alkyl chains of guanidinium lipids. Although two carboxylate groups in *cis*-1,2-cyclohexanedicarboxylate are located close to each other, but their orientations are far from parallel. Since stable complexation between the guanidinium and carboxylate requires a planar geometry, the maximized functional interaction is not compatible with the best chain packing. Two carboxylate

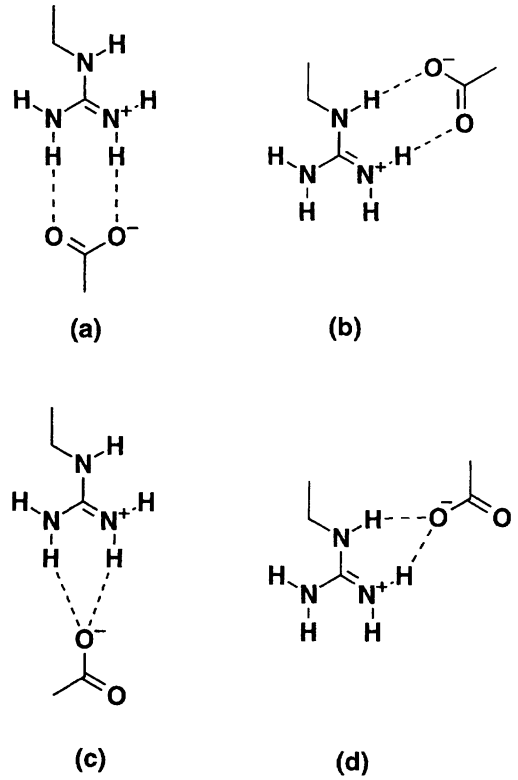

Fig. 8. Modes of interaction between guanidinium and carboxylate functions (Refs. 29 and 30).

groups in 1,1-cyclohexanediacetate are directed far apart, and the alkyl chain is packed even more loosely. These model considerations are in qualitatively good agreement with the observed results concerning the MG and DG(C_1) monolayers. The packing models (Fig. 7) based on the planar binding conformation can explain the order of the molecular areas of the guanidinium monolayers (phthalate <*cis*-1,2-cyclohexanedicarboxylate < 1,1-cyclohexanediacetate, Fig. 4). It is clear that the distance and relative orientation of the carboxylate groups in templates are important factors for determining the molecular packing in monolayers.

Mode of Interaction of Guanidinium Monolayers with Linear Dicarboxylates. Although we discussed the MM2 computational results of only three dicarboxylates in the preceding section, the conclusion which we obtained can be extended to other polycarboxylates. For example, linear dicarboxylates (group 1) expand the guanidinium monolayers, depending on the methylene length between the carboxylate groups. It can be explained by considering the difference in the distance between the carboxylate groups. However, the actual situation may not be that simple. In some cases, the planar conformation of the host–guest binding and the maintenance of the molecular packing in the monolayer are not compatible. In some cases, the maintenance of the best chain packing together with the planar conformation of the host–guest interaction is not compatible, and monolayers may rather maintain their chain packing at the expense of the planar host–guest binding. We already found a lower binding efficiency of malonate towards the DG(C_1) monolayer (Table 1). It might reflect a diminished binding to avoid a lesser molecular packing, because one methylene spacer is not long enough to set two carboxylate groups in a parallel orientation. An increasing spacer length would allow the dicarboxylates to accomplish an effective binding with the monolayer due to a larger conformational freedom. In fact, the binding efficiency to the DG(C_1) monolayer increased as the spacer length of the dicarboxylates increased.

However, we must not forget the fact that the molecular area also increased as the spacer methylene is elongated from malonate to adipate as can be seen in Fig. 3. Clearly, the alkyl-chain packing becomes looser upon complexation with dicarboxylates with longer methylene spacers. This implies that the host–guest interaction of the guanidinium/carboxylate complex is maintained only at the expense of a deteriorated chain alignment. The methylene spacer is not flexible enough to allow the maximum chain packing. Conversely, we can raise the possibility of controlling the molecular packing of guanidinium monolayers by choosing appropriate dicarboxylate guests. We have performed an AFM observation and an electron diffraction analysis of the DG(C_1) monolayer that is complexed with linear dicarboxylates.[31] The monolayer morphology is clearly affected by the kind of bound dicarboxylates. The binding of dicarboxylates with shorter methylene spacers converts the amorphous DG(C_1) monolayer to a crystalline one.

Oxalate gave unique FT-IR results. It is a rigid molecule in which two carboxylate groups are connected directly in the opposite directions. If two guanidinium amphiphiles bind to the two carboxylate groups through hydrogen bonding in a manner similar to the other dicarboxylates, the alkyl chains would extend to the opposite directions (Fig. 9a). This arrangement does not, of course, agree with the observed fact that the monolayer is closely packed in the condensed phase with limiting area comparable to the theoretical cross-sectional area of a single alkyl chain. More plausible binding structures include asymmetric complexes in which hydrogen bonding is formed at one side of the oxalate, and the second carboxylate is neutralized by either sodium cation (Fig. 9b) or by the guanidinium cation (Fig. 9c). Non-hydrogen bonded ion pairing between the monolayer and the carboxylate (Fig. 9d) could be an additional candidate. Among these possibilities, motif b is excluded by XPS data, which reveal the formation of a 2 : 1 complex and the absence of a Na^+ ion. The FT-IR data show that two types of carboxylate groups exist, one in the hydrogen-bonded form and the other in the non-hydrogen bonded form, indicating that motif d is not appropriate. Therefore, the most probable binding motif is model c, where one guanidinium binds to oxalate through hydrogen bonding, and another guanidinium exists as the counter ion of the other carboxylate group in oxalate.

Conclusions

Guanidinium monolayers interact with aqueous polycarboxylates most effectively through a combination of hydrogen bonding and an electrostatic interaction. This interaction requires the planar geometry of the complementary functions

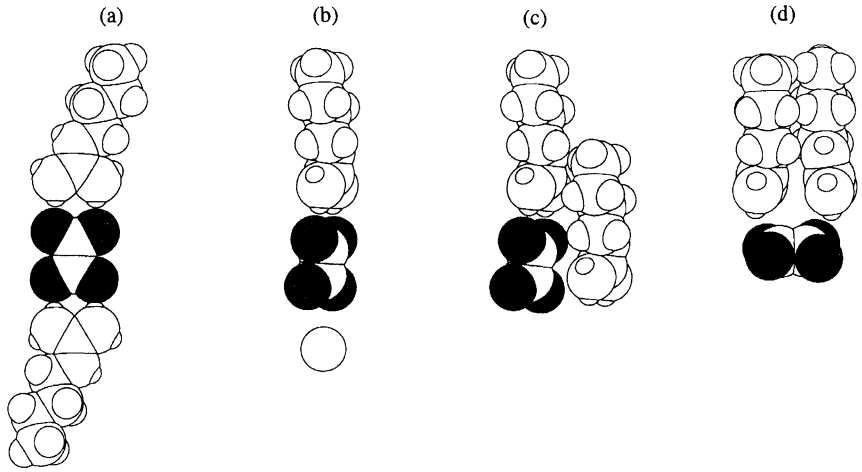

Fig. 9. Mode of interaction of alkyl guanidinium and oxalate; a: hydrogen-bonded motif at two carboxylate sites, b: 1 : 1 complex with one hydrogen-bonded carboxylate, c: one hydrogen-bonded carboxylate and one non-hydrogen-bonded carboxylate, d: two non-hydrogen-bonded carboxylates. Carboxylate oxygen atoms are shaded.

in order to maximize the hydrogen bonding. This requirement is not necessarily compatible with the best alkyl chain packing. The chain packing may not be optimized when the planar host–guest arrangement is maintained, as shown by an incremental expansion of the guanidinium monolayer with increasing methylene lengths in the linear dicarboxylate. The planar functional arrangement is impossible for an oxalate guest, and alkyl-chain packing is maintained by modifying the mode of interaction between the guanidinium and carboxylate. The influence of the relative orientation and the disposition of the carboxylate groups on the monolayer packing has been similarly observed for other polycarboxylates: phthalate, *cis*-1,2-cyclohexanedicarboxylate, and 1,1-cyclohexanediacetate.

In summary, we established in this study that aqueous polycarboxylates were specifically bound to guanidinium monolayers. We have already shown that a specific disposition of the monolayer components is realized through complementary hydrogen bonding with aqueous guests.[13] The present results indicate that the carboxylate/guanidinium pair is advantageous for this purpose. Polycarboxylates are versatile in molecular structure and may be synthesized relatively easily. We can look forward to the preparation of new types of molecular patterning by using polycarboxylate guests.

The authors thank Dr. Xiao Cha for a helpful discussion concerning the interpretation of the FT-IR spectra and Mr. Mitsuhiko Onda for assistance in the molecular model calculation.

References

1) F. Vögtle, "Supramolecular Chemistry," John Wiley & Sons, Chichester (1991).

2) J.-H. Fuhrhop and J. Koning, "Membrane and Molecular Assemblies, The Synthetic Approach," Royal Soc. Chem., London (1994).

3) T. Kunitake, *Angew. Chem., Int. Ed. Engl.*, **31**, 709 (1992).

4) A. Ulman, "An Introduction to Ultrathin Organic Films from Langmuir–Blodgett to Self-Assembly," Academic Press, San Diego (1991).

5) R. H. Tredgold, "Order in Thin Organic Films," Cambridge University Press, New York (1994).

6) a) D. Y. Sasaki, K. Kurihara, and T. Kunitake, *J. Am. Chem. Soc.*, **113**, 9685 (1991); b) D. Y. Sasaki, K. Kurihara, and T. Kunitake, *J. Am. Chem. Soc.*, **114**, 10994 (1992); c) D. Y. Sasaki, M. Yanagi, K. Kurihara, and T. Kunitake, *Thin Solid Films*, **210/211**, 776 (1992).

7) T. Kawahara, K. Kurihara, and T. Kunitake, *Chem. Lett.*, **1992**, 1839.

8) a) Y. Honda, K. Kurihara, and T. Kunitake, *Chem. Lett.*, **1991**, 681; b) K. Kurihara, K. Ohto, Y. Honda, and T. Kunitake, *J. Am. Chem. Soc.*, **113**, 5077 (1991).

9) a) K. Kurihara, K. Ohto, Y. Tanaka, Y. Aoyama, and T. Kunitake, *Thin Solid Films*, **179**, 21 (1989); b) K. Kurihara, K. Ohto, Y. Tanaka, Y. Aoyama, and T. Kunitake, *J. Am. Chem. Soc.*, **113**, 444 (1991).

10) Y. Ikeura, K. Kurihara, and T. Kunitake, *J. Am. Chem. Soc.*, **113**, 7342 (1991).

11) a) X. Cha, K. Ariga, M. Onda, and T. Kunitake, *J. Am. Chem. Soc.*, **117**, 11833 (1995); b) X. Cha, K. Ariga, and T. Kunitake, *Chem. Lett.*, **1996**, 73.

12) K. Taguchi, K. Ariga, and T. Kunitake, *Chem. Lett.*, **1995**, 701.

13) Y. Oishi, Y. Torii, M. Kuramori, K. Suehiro, K. Ariga, K. Taguchi, A. Kamino, and T. Kunitake, *Chem. Lett.*, **1996**, 411.

14) B. Springs and P. Haake, *Bioorg. Chem.*, **6**, 181 (1977).

15) D. D. Perrin and W. L. F. Armarego, "Purification of Laboratory Chemicals," 3rd ed, Pergamon, Oxford (1988).

16) R. A. B. Bannard, A. A. Casselman, and W. F. Cockburn, *Can. J. Chem.*, **36**, 1541 (1958).

17) M. Onda, K. Yoshihara, H. Koyano, K. Ariga, and T. Kunitake, *J. Am. Chem. Soc.*, **118**, 8524 (1996).

18) A. Kamino, K. Taguchi, H. Koyano, K. Ariga, and T. Kunitake, manuscript in preparation.

19) Analogous guanylating agents, *N,N'*-diacylated pyrazole-1-carboxamidines, are reported. a) M. S. Bernatowicz, Y. Wu, and G. R. Matsueda, *Tetrahedron Lett.*, **34**, 3389 (1993); b) B. Drake, M. Patek, and M. Lebl, *Synthesis*, **1994**, 579.

20) M. S. Bernatowicz, Y. Wu, and G. R. Matsueda, *J. Org. Chem.*, **57**, 2497 (1992).
21) A. Müller, *Proc. R. Soc. London, Ser. A*, **A114**, 542 (1927).
22) N. F. Hall and M. R. Sprinkle, *J. Am. Chem. Soc.*, **54**, 3469 (1932).
23) T. Kajiyama, H. Kozuru, Y. Takashima, Y. Oishi, and K. Suehiro, *Supramol. Sci.*, **2**, 107 (1995).
24) Y. Oishi, T. Kato, M. Kuramori, K. Suehiro, K. Ariga, A. Kamino, H. Koyano, and T. Kunitake, *Chem. Lett.*, **1996**, 857.
25) K. Kurihara, T. Kawahara, D. Y. Sasaki, K. Ohto, and T. Kunitake, *Langmuir*, **11**, 1408 (1995).
26) L. J. Bellamy, "The Infrared Spectra of Complex Molecules," 3rd ed, Chapman and Hall, London (1973), Chap. 10.
27) B. Brzezinski, J. Olejnik, and G. Zundel, *J. Chem. Soc., Faraday Trans.*, **90**, 1095 (1994).
28) L. J. Bellamy, "The Infrared Spectra of Complex Molecules," 3rd ed, Chapman and Hall, London (1973), Chap. 12.
29) D. M. Salunke and M. Vijayan, *Int. J. Peptide Protein Res.*, **18**, 348 (1981).
30) Y. Yokomori and D. J. Hodgson, *Int. J. Peptide Protein Res.*, **31**, 289 (1988).
31) T. Kato, M. Kuramori, Y. Oishi, K. Suehiro, K. Ariga, A. Kamino, H. Koyano, and T. Kunitake, *Rept. Prog. Polym. Phys. Jpn.*, in press.